Analysis and Design of a 3–26 GHz Low-Noise Amplifier in SiGe HBT Technology

Prabir K. Saha, Subramaniam Shankar, Rob Schmid, Richie Mills and John D. Cressler
School of Electrical and Computer Engineering, 777 Atlantic Drive, N.W.,
Georgia Tech, Atlanta, GA 30332-0250 USA
Email : prabir@gatech.edu / (404) 514-3052

***Abstract*—The analysis and design of a wideband silicon-germanium (SiGe) heterojunction bipolar transistor (HBT) low noise amplifier (LNA) is presented. Resistive shunt-shunt feedback is employed to achieve wideband gain and matching characteristics and it is shown that the addition of small reactive elements can extend the bandwidth of the amplifier significantly. Measured data for the LNA, implemented in a 130-nm SiGe BiCMOS technology, show 9 dB gain with less than 1.0 dB variation across 3-26 GHz, and input and output return losses better than -10 dB over the entire bandwidth. The measured noise figure (NF) is less than 5 dB from 3-18 GHz and rises to only 6.5 dB at 24 GHz. In addition, the amplifier exhibits excellent linearity performance, with a input-referred third-order intercept point (IIP3) of 5.8 dBm and input-referred 1 dB compression point (P1dB) of -5.6 dBm. This SiGe amplifier occupies 0.48 mm^2 (including pads) and consumes 33 mW of power while operating off a 3.3 V supply.**

I. Introduction

Wideband low noise amplifiers are critical components for virtually all broadband communications systems. In recent years, allocation of the 3-10 GHz frequency band for ultra-wide band (UWB) applications has fueled tremendous interest in this domain [1] and resulted in a flurry of publications [2], [3], [4], [5]. Wideband LNAs also find extensive application in instrumentation systems, as well as optical communications and software defined radios. An amplifier with good matching and noise performance is essential to all such applications.

Known wideband amplifiers can be categorized into four different topologies. Narrow-band concepts can be extended for broadband applications by having higher-order matching networks at the input and output. Inclusion of a large number of inductances and capacitances becomes prohibitively costly, however, in terms of chip area and the inherent low quality-factor (Q) of such passive elements for monolithic implementation in silicon degrades the noise performance. Common-base or common-gate amplifiers provide inherent wideband characteristics but suffer from high noise figure. Distributed amplifiers, while being the best choice for large bandwidths, suffer from large die area and high power consumption. Resistive feedback LNAs, on the other hand, provide a compact solution with good wideband noise performance and low power consumption. Several implementations covering the 3-10 GHz UWB band can be readily found in the literature. Traditional inductor-less resistive feedback LNAs provide a very compact solution, but at the same time have limited maximum operating frequency. In the present paper, we investigate the limits of the resistive-feedback LNA topology and demonstrate how its operating bandwidth can be further extended by using small inductances, with very little area penalty.

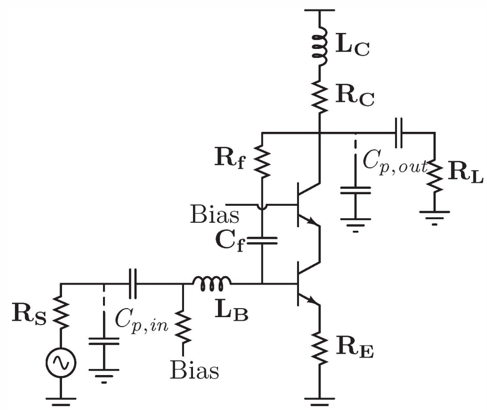

Fig. 1. Schematic of resistive feedback LNA with reactive components for improved matching.

There has been some discussion in the literature along similar lines in recent years [6], in which use of a π-matching network at the input has been shown to improve input matching. In the present paper, the effects of the matching network on the input matching, gain and noise are analyzed in the context of a SiGe amplifier, for the first time. A design approach that exploits the parasitics in the circuit to implement the matching network and improves performance is then presented. Theoretical analysis of the impact of reactive matching on resistive feedback amplifier is presented in section II. Measurement results and a comparison with other published data are given in section III, followed by a summary.

II. Analysis of a Resistive Feedback Amplifier with Reactive Matching

Fig. 1 shows the schematic of the resistive shunt-shunt feedback amplifier with reactive components for improved matching. Parasitic capacitances at the input and the output nodes are also included. At low frequency, under the assumption that the device input impedance is much higher than R_f, straightforward analysis yields expressions for the input and output resistances:

$$R_{in} = \frac{R_f + R_L^{'}}{1 + g_m R_L^{'}} \tag{1}$$

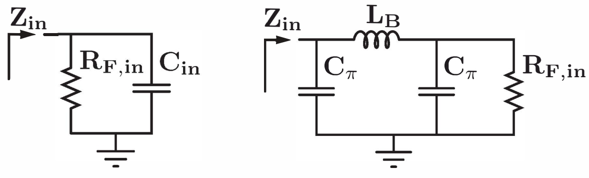

(a) (b)

Fig. 2. Equivalent small-signal representation of input impedance: (a) without matching and (b) with π-matching network.

$$R_{out} = R_C||(\frac{R_f + R_S}{1 + g_m R_S}) \tag{2}$$

where $R_L' = R_C||R_L$. In the following analysis, we examine how the capacitances cause the impedances to depart from their ideal values and how this situation can be improved by designing a modified matching network. The effects of reactive matching on gain and noise is also considered.

A. Input Matching

The assumption of very high device input impedance breaks down at high frequencies. Device input capacitance (C_π), together with parasitic capacitances present at the input node, moves the input impedance (Z_{in}) away from its ideal value. The input impedance can be expressed as

$$Z_{in} = R_{F,in}||(\frac{1}{j\omega C_{in}}) \tag{3}$$

where $R_{F,in} = (R_f + R_L')/(1 + g_m R_L')$ and $C_{in} = C_\pi + C_{p,in}$; $C_{p,in}$ being the parasitic capacitances associated with the input node (Fig. 1). The small-signal equivalent circuit is shown in Fig. 2(a). $R_{F,in}$ is often designed to be equal to R_S, which is usually 50 Ω for RF systems. The range of frequencies over which S_{11} is less than 10 dB can be taken as a reasonable measure for good input matching,

$$20.log\left|\frac{1/R_S - 1/R_{F,in} - j\omega C_{in}}{1/R_S + 1/R_{F,in} + j\omega C_{in}}\right| < -10 \tag{4}$$

which can be expressed as

$$\omega^2 < (-1 + 2.44/r - 1/r^2).\frac{1}{(R_S C_{in})^2} \tag{5}$$

where $r = R_{F,in}/R_S$. From (5), it can be determined that the input matching bandwidth is maximized for $r = 0.82$. However, a smaller $R_{F,in}$ would also mean a higher noise contribution from the feedback resistor and hence will degrade overall amplifier noise figure.

The input matching bandwidth can be extended if an inductor (L_B) is added at the base of the input device. Fig. 2 (b) shows the transformed equivalent circuit as far as the input impedance is concerned. L_B separates the device capacitance (C_π) from the parasitic capacitances and forms a π-matching network. For the following analysis, it is assumed that the π network is symmetric. This can be achieved by adding capacitance to the input node, if necessary. Fig. 3 shows how the S_{11} magnitude compares to the standard resistive feedback

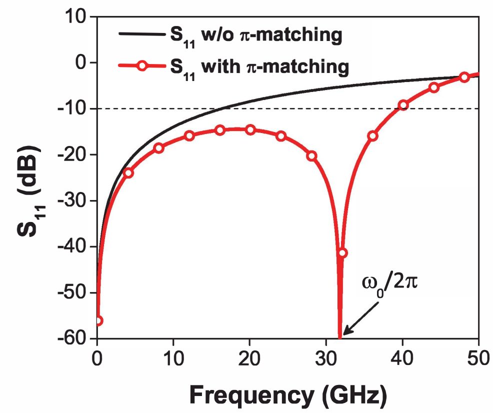

Fig. 3. S_{11} with and without the π matching network at the input.

amplifier. In addition to DC, the π-matching network provides perfect matching at $\omega_0/2\pi$. The frequency ω_0 can be easily found by noting the frequency at which the reactive part of Z_{in} goes to zero,

$$\omega_0 = \sqrt{\frac{2}{L_B C_\pi} - \frac{1}{R_{F,in}^2 C_\pi^2}} \tag{6}$$

If ω_0 is not too far away from DC, S_{11} stays below -10 dB for all intermediate frequencies and the matching bandwidth is thus greatly increased.

B. Gain

The input matching network forms a third-order low-pass filter and there is another pole at the output. An exact analytical expression for small-signal gain ($A_V = V_{out}/V_S$) is too cumbersome to provide much insight. Under the assumption of a symmetric π-matching network ($C_\pi = C$) and $R_S = R_{F,in} = \sqrt{L_B/C_\pi} = R$ (where $R_{F,in} = (R_f + R_L')/(1 + g_m R_L')$), the small-signal gain can be expressed as,

$$A_V \approx \frac{1/2}{(1+s\frac{L}{R}+s^2LC)}.\frac{-g_m(R_F||R_L')}{1+s(R_F||R_L')C_{out}} \tag{7}$$

where $R_L' = R_C||R_L$. The key difference between this result and a purely resistive feedback amplifier lies in the input matching network. The device input capacitance (C_π) is absorbed into the π network. A first-order pole at the input ($1/(R_S||R_{F,in}||\frac{1}{j\omega C})$) is replaced by a second-order low pass filter with a cut-off frequency ($1/\sqrt{LC}$), which is typically higher and thus improves the overall frequency response. A comparison of the frequency response of S_{21} with and without the matching network is shown in Fig. 4.

C. Noise

The small-signal model of a purely resistive-feedback LNA, including all significant sources of noise, is shown in Fig. 5. Noise contributions from R_E and r_b are included, but the effects of r_b are excluded from impedance calculations

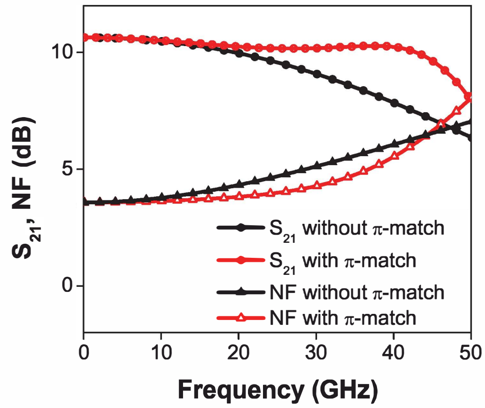

Fig. 4. Effect of input matching network on S_{21} and noise figure.

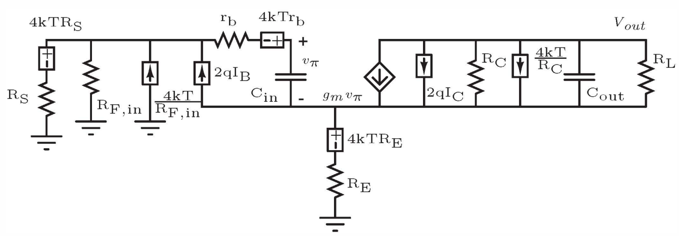

Fig. 5. Small-signal model of resistive feedback amplifier including noise sources.

to reduce complexity. Equivalent input referred noise can be expressed as,

$$
\begin{aligned}
v_{ni}^2/\Delta f = \quad & 4kT(R_S + r_b + R_E) + (\tfrac{4kT}{R_{F,in}} + 2qI_B) \\
& .(R_S||R_F)^2 + 2qI_B.R_E^2 \\
& + \tfrac{4kT/R_C + 2qI_C}{g_m^{'\,2}} \left|1 + j\omega(R_S||R_{F,in})C_\pi^{'}\right|^2 \qquad (8)
\end{aligned}
$$

where $g_m^{'} = g_m/(1 + g_m R_E)$ and $C_\pi^{'} = C_\pi/(1 + g_m R_E)$ and noise figure can be calculated as $v_{ni}^2/(4kTR_S)$. It can be readily seen from (8) that low frequency noise can be reduced by reducing R_E and increasing $R_{F,in}$, as expected.

With increasing frequency, collector current shot noise and load resistor thermal noise contributions increase, which is captured in the last term of the Eqn. (8). This is due to the pole associated with the input node of the amplifier. Signals traveling through the pole get reduced in magnitude beyond the 3-dB cutoff frequency, but noise originating after the location of the pole ($2qI_C$ and $4kT/R_C$) is not affected. As a result, the signal-to-noise ratio (SNR) is degraded.

As discussed above, inclusion of the π matching network moves the input pole to higher frequency and hence increases the frequency at which the noise figure rapidly increases. In other words, the π-matching networks helps to maintain a flat noise figure response across frequency, as shown in Fig. 4.

III. Measurement Results

An LNA demonstrating this design approach was implemented in a 130-nm SiGe BiCMOS process with 7 metal layers. The SiGe HBTs have a peak f_T of 200 GHz. The devices were biased well below their peak f_T current density to optimize noise performance. The schematic is shown in Fig. 1. An emitter degeneration resistor (R_E) was included to improve linearity. The effects of emitter degeneration can be easily included in the above analysis on matching performance by simply modifying the transconductance (g_m) and input capacitance of the device (C_π) by the degeneration factor ($1/(1 + g_m R_E)$). Parasitic capacitances at the input node ($C_{p,in}$, due to the bondpad and decoupling capacitor), along with the base inductance (L_B) and the device input capacitance (C_π), forms the input π-matching network. The implemented π network is not perfectly symmetric, but still results in a substantial performance improvement. A gain peaking inductor (L_C) was added to further boost the gain at high frequencies and flatten the gain response across frequency.

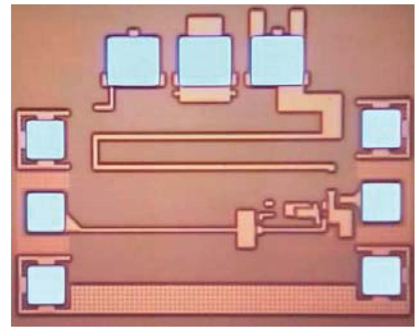

Fig. 6. Die microphotograph of the SiGe LNA.

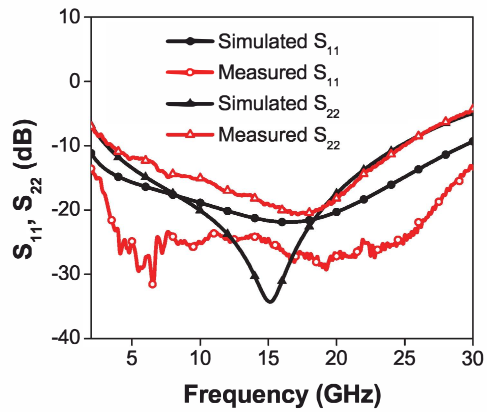

Fig. 7. Measured input and output reflection coefficients (S_{11} and S_{22}) of the SiGe LNA.

A die photomicrograph of the LNA is shown in Fig. 6. The die area including bondpads is 0.8 μm x 0.6 μm. This LNA is entirely monolithic and does not require any external bias-tee or RF-choke.

Measured and simulated S-parameters are shown in Fig. 7 and Fig. 8. The measured gain (S_{21}) is nominally 9 dB (Fig. 8) and exhibits a very flat frequency response, with less than 1 dB variation over a frequency range of 2-30 GHz. The measured S_{11} is less than -10 dB over 2-30 GHz. S_{22}, as shown in Fig. 7, is better than -10 dB over 3-26 GHz. It should be noted

TABLE I
PERFORMANCE SUMMARY AND COMPARISON WITH OTHER PUBLISHED WIDEBAND LNAS

	BW (GHz)	S_{21} (dB)	Gain var. (dB)	NF (dB) (3-10 GHz)	NF (dB)	IIP3 (dBm)	P1dB (dBm)	Power (mW)	Die Size (mm^2)	Technology
This work	3–26	9	< 1	< 4.5	< 6.5	5.8	-5.6	33	0.48	130-nm SiGe BiCMOS
[7]	0.1–20	11.2	3	–	3.3–5.5	-2.5	–	20.4	0.35	90-nm CMOS
[6]	1.6–28	9.6	2.2	2.92–3.23	2.92–4.4	4	-9	21.6	0.139	90-nm CMOS
[8]	0–22.1	9.2	3	–	4.3–6.6	-2.67	–	8.4	0.131	90-nm CMOS
[9]	1–25	11.5	3	–	3.5–4.5	15.5	4.5	900	1.44	200-nm GaN
[4]	3–10	20	1	3.05–4.5	–	-11.7	–	42.5	0.52	200-nm SiGe

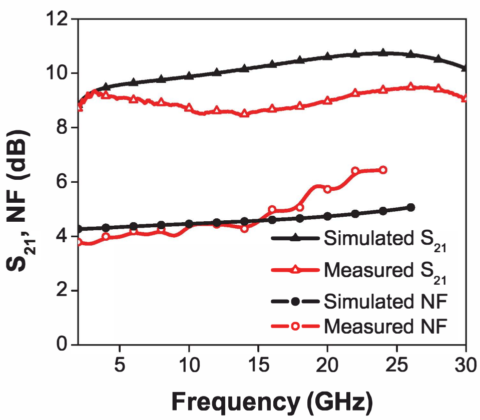

Fig. 8. Gain (S_{21}) and noise figure vs. frequency of the SiGe LNA: comparison of measured and parasitic-extracted simulation results.

that the low frequency limit of matching is imposed by the DC blocking networks at the input and the output and can be improved by increasing the size of the DC blocking capacitors, at the cost of increased die area and parasitics.

Simulated and measured noise figure are shown in Fig. 8. The measured noise figure remains below 4.5 dB over 2-14 GHz. Beyond 18 GHz, the measured data did not match simulation very well, but the noise figure remains under 6.5 dB up to 24 GHz. The measured input IP3 and 1-dB compression point of the LNA is 5.8 dBm and -5.6 dBm, respectively. Emitter degeneration was used to improve linearity, at the cost of increased noise figure. Clearly, the noise performance of the LNA can be improved for a less stringent linearity requirement. The amplifier draws 10 mA from a 3.3 V supply.

A comparison with other published data is presented in Table I. The SiGe LNA implemented in this work excels in terms of gain flatness over bandwidth of operation and in linearity performance. The noise figure is slightly higher than some of the other designs, but that is due to its inherent tradeoff with linearity. It should be noted that this LNA does not require any external component to function. In contrast, [6] requires an external RF choke. Table I shows that overall performance of this wideband SiGe LNA is competitive with other state-of-the-art designs, in either CMOS or III-V platforms, some of which are implemented in more aggressive (costly) technology nodes.

IV. SUMMARY

The analysis and design of a wideband SiGe low noise amplifier (LNA) was presented. It was shown that by adding small inductors into the scheme of resistive feedback amplifier design, matching can be greatly improved. The effects of a π-matching network at the input of the LNA on matching, gain and noise performance was analyzed theoretically. The design approach of combining reactive matching with resistive feedback improves performance compared to a traditional shunt-shunt resistive feedback, at the cost of slightly increased die area.

ACKNOWLEDGMENT

The authors are grateful to A. Cardoso, T. Wilcox, and J. Papapolymerou for their contributions.

REFERENCES

[1] D. Porcino *et al.*, "Ultra-Wideband Radio Technology: Potential and Challenges Ahead," *IEEE Comm. Mag.*, vol. 41, no. 7, pp. 66–74, Jul. 2003.

[2] Y. Park *et al.*, "A Very Low Power SiGe LNA for UWB Application," in *Tech. Dig. IEEE Int. Microwave Symp.*, Jun. 2005, pp. 1041–1044.

[3] Y. Lu *et al.*, "A 1.8–3.1 dB Noise Figure (3–10 GHz) SiGe HBT LNA For UWB Applications," in *Proc. IEEE RFIC Symp.*, Jun. 2006, pp. 45–49.

[4] J. Lee *et al.*, "Analysis and Design of an Ultra-Wideband Low-Noise Amplifier Using Resistive Feedback in SiGe HBT Technology," *IEEE TMTT*, vol. 54, no. 3, pp. 1262–1268, Mar. 2006.

[5] Y. Lin *et al.*, "3–10-GHz Ultra-Wideband Low-Noise Amplifier Utilizing Miller effect and Inductive Shunt–Shunt Feedback Technique," *IEEE TMTT*, vol. 55, no. 9, pp. 1832–1843, Sep. 2007.

[6] H. Chen *et al.*, "Analysis and Design of a 1.6–28-GHz Compact Wideband LNA in 90-nm CMOS Using a π-Match Input Network," *IEEE TMTT*, vol. 58, no. 8, pp. 2092–2104, Aug. 2010.

[7] M. Chen and J. Lin, "A 0.1–20 GHz Low-Power Self-Biased Resistive-Feedback LNA in 90 nm Digital CMOS," *IEEE MWCL*, vol. 19, no. 5, pp. 323–325, May 2009.

[8] M. Okushima *et al.*, "A DC-to-22 GHz 8.4mW compact dual-feedback wideband LNA in 90 nm digital CMOS," in *Proc. IEEE RFIC Symp.*, Jun. 2009, pp. 295–298.

[9] M. Chen *et al.*, "A 1–25 GHz GaN HEMT MMIC Low-Noise Amplifier," *IEEE MWCL*, vol. 20, no. 10, pp. 563–565, Oct. 2010.